Influence of Structural Elasticity on Trailing Edge Noise

Li Chen[1] and Nicole Kessissoglou[2]

[1] Maritime Division, Defence Science and Technology Organisation, Melbourne, Australia

[2] School of Mechanical and Manufacturing Engineering, UNSW Australia, Sydney, Australia

ABSTRACT

For an airfoil, a hydrofoil or a control surface in high Reynolds number flow, the noise generated by the turbulent boundary layer is scattered by the trailing edge and then radiated efficiently. This is an important broadband noise problem, particularly at high frequencies. For aeronautical applications, estimations of trailing edge noise are mainly based on the assumption of rigid surfaces. In underwater applications, the foils may no longer be considered as rigid. The trailing edge noise is then the result of the vibro-acoustic coupling of the flow and the foils. In this paper, the influence of structural elasticity on trailing edge noise generation is investigated. The turbulent flow loading on a 2D hydrofoil is modelled using a Reynolds-Averaged-Navier-Stokes based computational fluid dynamics approach. The fluid loading is then applied to the bending wave equation of a thin plate to predict elastic edge noise. Rigid edge noise is also predicted using the flow loading combined with a Green's function. Four different materials are examined in this study.

Keywords: flow noise, trailing edge noise, hydrofoil, fluid-structure interaction, structural elasticity, I-INCE Classification of Subjects Number(s): 21.6.5.

1. INTRODUCTION

Mechanisms leading to the generation of flow noise are complex and involve a wide range of physical phenomena (1,2,3,4,5,6). A comprehensive description of the mechanisms associated with flow induced noise is given by Crighton (7). The propagation of flow-induced noise is described by Lighthill's inhomogeneous wave equation (8,9). The well-known Lighthill tensor is related to the turbulent flow and the so-called turbulence quadrupole. Different methods to calculate quadrupole noise are given by Wang et al. (1,11). For a low Mach number wall-bounded flow, the radiation of quadrupole sources can be related to the surface pressure fluctuation beneath a turbulent boundary layer through a proper Green's function (3,12,13). However, sound generated by turbulent flow over an infinite surface has quadrupole radiation characteristics; therefore only turbulent eddies with a length scale near the acoustic wavenumber will radiate. However, with a termination of the surface, such as a trailing edge, the turbulence-induced noise will radiate with a dipolar pattern, allowing turbulence eddies with smaller scales to radiate more efficiently. The radiated turbulence noise generated for low-Mach-number flow by the trailing edge of hydrofoils of a semi-infinite chord with finite spanwise dimension is due to scattering.

The flow-induced noise scattered by the trailing edge of an airfoil, a hydrofoil or a flow control surface can be an important broadband noise problem, particularly at high frequencies. The edge scatters the inefficient quadruple turbulence source into dipole radiation and converts turbulence eddies of small scales into sound. For aeronautical applications, estimations of trailing-edge noise are mainly based on the assumption of rigid surfaces. Previous research on the passive treatment of a trailing edge to reduce the edge noise can be found in Refs. (14,15). In underwater applications, however, the surrounding water is a heavy fluid and applies a large external force on the foils. In this case, the influence of the heavy fluid loading will change the mechanical properties of the foils, so that the foils can no longer be considered as rigid (16). The trailing edge noise is then the result of the vibro-acoustic coupling of the flow and the foils. The elasticity of the foil needs to be taken into account in the trailing edge noise prediction. Also the foil can be more easily excited by the large flow loading. Flexural waves will be generated in the structure and radiated as sound by scattering at structural discontinuities.

In this paper, the influence of structural elasticity on trailing edge noise generation is investigated. The turbulent flow loading on a 2D hydrofoil is modelled based on the Reynolds Averaged Navier Stokes (RANS) equations using computational fluid dynamics (CFD). The fluid loading is applied to the bending wave equation of a thin plate to predict the edge noise. The effect of the noise scattering at the plate edge for different materials is described.

2. Trailing Edge Noise

2.1 Noise from a Rigid Edge

Sound generated by turbulent flow over a large surface has quadrupole radiation characteristics. Only turbulent eddies with length scales near the acoustic wavenumber will radiate. However, with a termination of the surface, such as a trailing edge, the turbulence-induced noise will radiate with a dipolar pattern, allowing turbulence eddies with smaller scales to radiate more efficiently. Such trailing edge noise is important, particularly for a low Mach number flow. The trailing edge of a hydrofoil of a semi-infinite chord with a finite spanwise dimension *L* is orientated as shown in Figure 1.

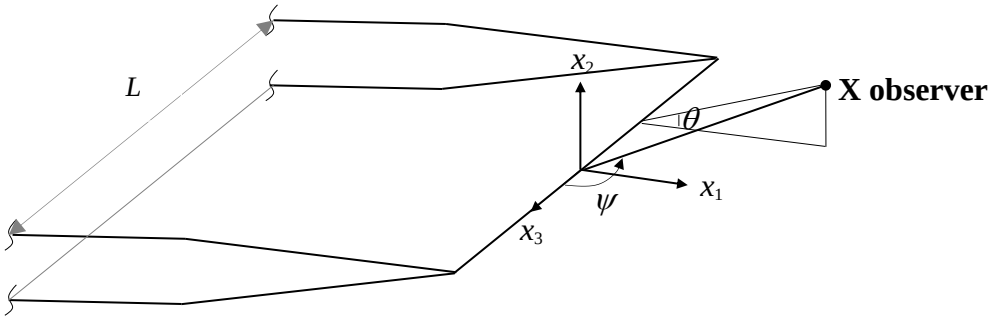

Figure 1 – Coordinates defining trailing edge noise from a half-foil

For a rigid edge, the spectrum of the noise Φ_{rigid} can be expressed in terms of the boundary layer wall pressure Φ_{pp} as (22)

$$\Phi_{\text{rigid}}(\mathbf{x},\omega) = \frac{\omega L \sin^2(\theta/2)\sin\psi}{2\pi c_0 |\mathbf{x}|^2} \Phi_{\text{pp}}(\omega) l_3 \tag{1}$$

where ω is the radian frequency and c_0 is the sound speed in the fluid. The spanwise correlation length scale of the pressure fluctuation is $l_3 = 2.1U_c/\omega$ where U_c is the convection velocity. $\mathbf{x}(x_1, x_2, x_3)$ is observation coordinates.

2.2 Noise from an Elastic Edge

When the foil is moving in water, the fluid loading is large. In this case, turbulence near the edge is expected to excite flexural waves in the structure. Trailing edge noise results from the fluid-structure interaction between the flow and the foil. Given that only a foil of a large aspect ratio is considered, the foil is assumed to be a thin flat plate in bending motion. Fluid loading affects the mechanical properties of the thin plate when the frequency is much less than the coincident frequency of the plate. The coincident frequency ω_c is defined as (22)

$$\omega_c = c_0^2 \sqrt{\frac{m}{B}} \tag{2}$$

where *m* is the mass per unit area, $B = Eh^3/12(1-\nu^2)$ is the bending stiffness of a flat plate of thickness *h*. *E* and ν are respectively the plate Young's modulus and Poisson's ratio. The fluid loading parameter ε is defined as (22)

$$\varepsilon = \frac{\rho_0 k_0}{m K_0^2} \equiv \frac{\rho_0}{\rho_s}\left(\frac{E}{12\rho_s c_0^2 (1-\nu)^2}\right)^{1/2} \tag{3}$$

The influence of the fluid loading becomes important when $\omega/\omega_c < \varepsilon^2$. The acoustic wavenumber is $k_0 = \omega/c_0$ and the in-vacuo bending wavenumber K_0 is defined as $K_0 = (m\omega^2/B)^{1/4}$. ρ_s and ρ_0 are respectively the density of the foil and the fluid. The displacement of the foil ξ under a pressure loading Δp due to turbulent boundary flow is governed by the inhomogeneous bending wave equation as (23)

$$\left\{B\left(\frac{\partial^2}{\partial y_1^2} + \frac{\partial^2}{\partial y_3^2}\right)^2 + m\frac{\partial^2}{\partial t^2}\right\}\xi = \Delta p\left(y_1, 0, y_3\right) \tag{4}$$

|**y**| represents the source coordinates with an orientation the same as the observation coordinate system. Furthermore, the displacement of the foil and the pressure loading are related by the y_2 component of momentum equation as follows

$$\rho\frac{\partial^2 \xi}{\partial t^2} = -\frac{\partial p}{\partial y_2}, \quad y_2 = 0 \tag{5}$$

Detailed solutions of Eq. (3) and Eq. (4) for a half-plate can be found in Howe (23). The noise scattered from the trailing edge of the elastic half-plate due to the turbulent flow is given by

$$\Phi_{\text{elastic}}(\mathbf{x}, \omega) = \frac{U_c L A_n^2 \sin^2\theta \sin\psi}{8\pi|\mathbf{x}|^2 c_0 \varepsilon^{(4n+1)}}\left(\frac{\omega}{\omega_c}\right)^{2n+1} \Phi_{\text{pp}}(\omega) l_3 \tag{6}$$

A_n and n are numerical constants depending on the boundary conditions at the trailing edge of the plate. For a free edge, $A_n = 1.097$ and $n = 0.2$. For a clamped edge, $A_n = 1.475$ and $n = -0.2$.

For an edge to be considered as a source of noise, the edge should be sufficiently rigid to be able to interact with the noise sources produced by the turbulence. This requires the plate bending wave length to be much greater than the length scale of the local turbulence eddies, which implies $K_0 \ll \omega/U_0$. Therefore the fluid loading will only become important in the range:

$$\left(\frac{U_0}{c_0}\right)^2 \le \frac{\omega}{\omega_c} < \varepsilon^2 \tag{7}$$

For many underwater applications, the flow Mach number given by $M = U_0/c_0$ where U_0 is the free stream velocity, is very small. For a steel plate of 5 mm thickness in water, the fluid loading parameter ε is around 0.1. This implies that for frequencies up to 830 Hz, Eq. (7) is satisfied and the fluid loading is important. For a different material from steel, there will be a wider range of frequencies satisfying Eq. (7), which is discussed in section 4. For underwater applications, the acoustic length scale is significantly larger than the length scale of the turbulence eddies. Also, to satisfy Eq. (7), the length scale of the bending wave has to be much larger than the scale of the turbulence eddies. Hence, the flow can be computed for a rigid plate and considered as incompressible.

2.3 Point Surface Pressure Spectrum

There are several methods to obtain the point surface pressure spectrum for a turbulent boundary layer flow, which depends on the turbulence statistics. As the focus of this study is on the effect of material elasticity on the trailing edge noise, an empirical model is adopted. A previous study by the first author (18) has shown that the empirical model proposed by Blake (13) based on their experimental data provides a reasonable comparison with the experimental data of Ref. (19). The model was improved by Ahn (20) based on the best fitting of the spectrum data in Blake (21) and is used in this study. The empirical model for the boundary layer wall pressure is given by

$$\Phi_{\text{pp}}(\omega) = \left(\frac{\tau_w^2 \delta^*}{U_0}\right)\frac{\left(2\pi 8.28 St^{0.8}\right)}{\left(1 + 4.1 St^{1.7} + 4.4\times 10^{-4} St^{5.9}\right)} \tag{8}$$

where δ^* and τ_w are respectively the displacement boundary layer thickness and wall shear stress.

The dimensionless frequency is

$$St = \frac{\omega \delta^*}{U_0} \tag{9}$$

3. SIMULATION OF TRAILING EDGE FLOW

Trailing edge noise can be related to the surface pressure fluctuation spectrum by a Green's function. The surface pressure fluctuation is a product of turbulent flow. Methods to predict the pressure spectrum include Direct Numerical Simulation (DNS) and Large Eddy Simulation (LES). However, these techniques are computationally expensive. For practical problems, a computationally efficient method is desirable. A Reynolds Averaged Navier Stokes (RANS) based approach predicts the pressure spectrum using the empirical model given by Eq. (8) to calculate the spectrum in this study. The model is developed from experimental data, and has been found to agree reasonably well with the more comprehensive RANS based model (18) which requires a detailed turbulence boundary layer mean flow and turbulence statistics. The pressure spectrum predicted using the comprehensive RANS based model shows very good agreement with the experimental data. Detailed validation of the comprehensive RANS based model can be found in Ref. (18), in which the detailed validation of the trailing-edge prediction using the hybrid model is also presented.

The computation of 2D turbulent flow over a NACA0015 foil was performed using FLUENT. The two-dimensional NACA 0015 hydrofoil investigated has a chord length C of 540mm and the trailing edge was truncated at 98% of the chord. The computational domain developed for the URANS analysis has a two-dimensional C-type control volume of dimension: $12C \times 4C$. A 'velocity inlet' boundary condition was applied four chord lengths upstream of the section's leading edge, while a 'symmetry' boundary condition was designated at $2C$ from the suction and pressure surface of the hydrofoil. An outflow boundary condition was implemented at seven chord lengths downstream of the trailing edge. The surfaces of the lift section were defined using a no-slip 'wall' boundary condition. The computational domain was discretized using pure quadrilateral cells with higher cell distribution allocated to the immediate wake region, as shown in Figure 2a. The foil was aligned parallel to the incoming flow. The flow was modelled using the RANS method, with turbulence modelled using the SST (Shear-Stress-Transport) k–ω model. The simulations were carried out with four different meshes to ensure grid independence. The simulations were carried out at the chord-based Reynolds number, $\mathrm{Re} = \rho UC/\mu$, varying between 1.407×10^6 - 6.019×10^6. To avoid repetition, the details of the CFD simulation, including mesh independence studies and model validations, can be found in previous work by Do et al. (25).

The flow field is shown in Figure 2b and 2c. The flow is always attached to the foil with a symmetrical pressure distribution. This ensures high confidence of the application of the empirical formula.

To characterize the boundary layer, the boundary layer displacement thickness near the trailing edge is widely used. It is also used as a critical length scale to define the dimensionless pressure spectrum in Eq. (8), as described in Ref. (21). The boundary layer displacement thickness is defined as

$$\delta^* = \int_0^\infty \left(1 - \frac{U(y)}{U_0}\right) dy_2 \tag{10}$$

where $U(y)$ is the velocity magnitude above the foil and y_2 is the coordinate normal to the wall. The calculated boundary layer displacement thickness and wall shear stress near the trailing edge as a function of Reynolds number are shown in Figure 3. It can be seen that with an increase in Reynolds number, the boundary layer becomes thinner (Figure 3a) and the wall shear stress is increased (Figure 3b).

4. RESULTS AND DISCUSSION

The surface pressure spectrum is obtained from the CFD simulation. The calculated surface pressure spectrum as a function of chord based Reynolds number is shown in Figure 4. The dimensionless pressure spectrums collapse on to the same curve due to the parameters used in the non-dimensionalised formula. The spectrum reaches a maximum value near $\omega\delta^*/U_0 = 0.3$ and shows complicated frequency dependence. This is reflecting the nature of a turbulent boundary layer. The

$\omega^{-0.7}$ dependence of the pressure spectrum is understood to be related to the motion of turbulence in the logarithmic region of the boundary layer. The parabolic behavior ω^2 in the low frequency range is a result of turbulence eddy convection in the viscous sub-layer (13).

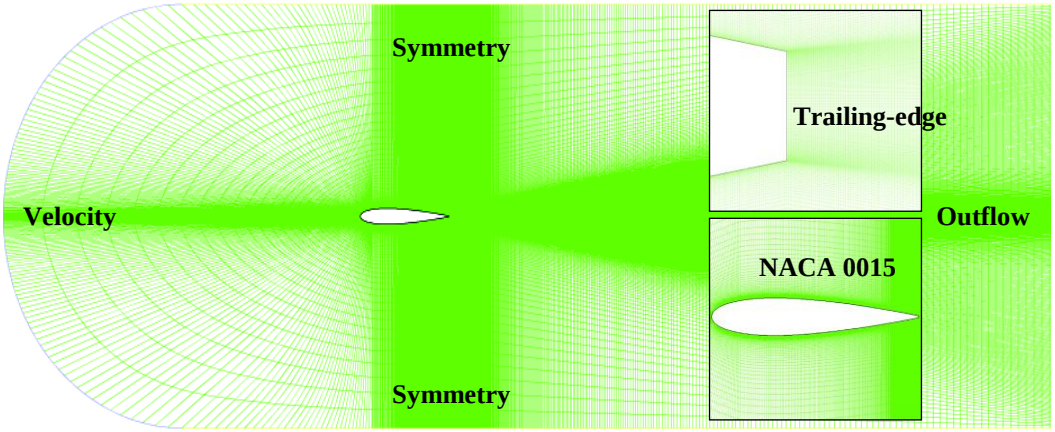

(a) Schematic diagram of the computational domain and boundary conditions

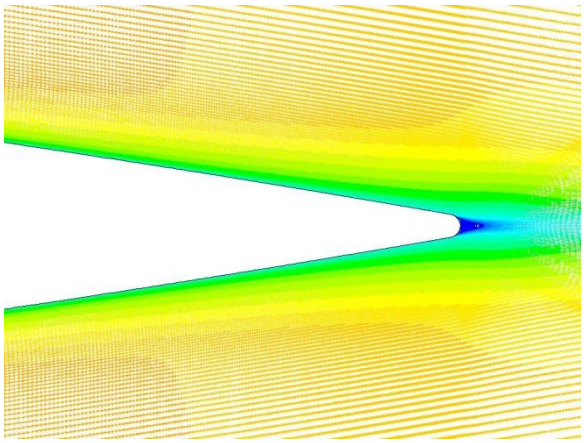

(b) Velocity field

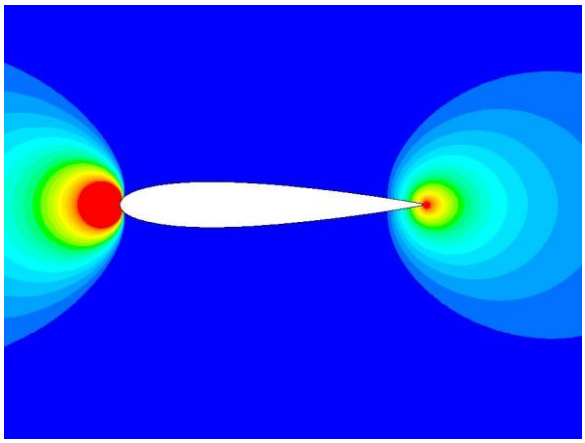

(c) Pressure contours

Figure 2 – Flow field over NACA0015 in water

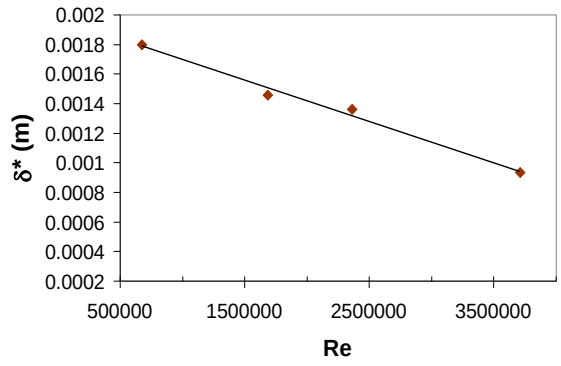

(a) Displacement thickness

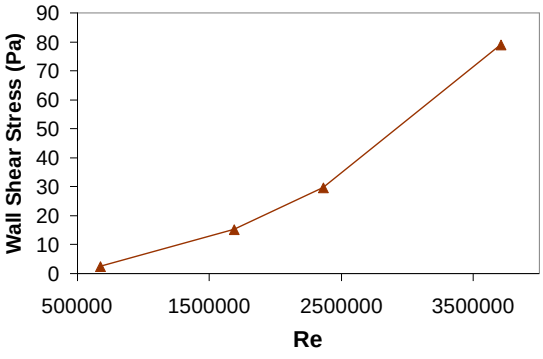

(b) Wall shear stress

Figure 3 – The boundary layer displacement thickness (a) and wall shear stress (b) as a function of chord based Reynolds number

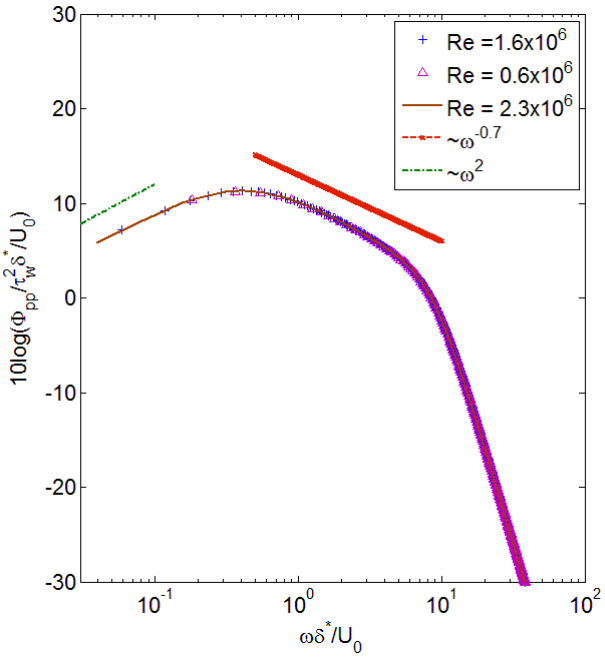

Figure 4 – Dimensionless surface pressure spectrum

The calculated pressure spectrum is then used in Eq. (1) for the rigid edge noise and in Eq. (6) to predict the trailing edge noise of different elastic materials. The chosen materials correspond to aluminium alloy, stainless steel, titanium alloy and tungsten. The calculated parameters for the four materials are listed in Table 1. Values for the Young's modulus and Poisson ratio are obtained from Ref. (26).

Table 1 – Summary of material parameters

Material	Bending stiffness B	Fluid loading parameter ε (Eq. 3)	Coincident frequency f_c (kHz) (Eq. 2)	Density (kg/m^3)
Aluminium alloy	102.28	0.4	90.7	2626
Stainless steel	275.28	0.1256	96	7905
Titanium alloy	154.88	0.2217	96	4470
Tungsten	488.28	1.4204	35.2	1900

The noise is calculated for a Reynolds number of $\mathrm{Re}=1.6\times10^6$ at the observation point $x_1=0,\ x_2=0,\ x_3=1.2$. The thickness of the foil is assumed to be h =2.5 mm. In this case, the Mach number of the flow is 0.0033. The use of a very flexible material such as rubber for the foil in water, the very high coincident frequency and small fluid loading parameter restrict the application of Eq. (6) to a very narrow frequency range. That is, the fluid loading only becomes important at very low frequencies as far as trailing edge noise is concerned. However, using aluminium alloy, stainless steel, titanium alloy and tungsten for the foil in water, Eq. (6) is applicable for a much wider frequency range. For aluminium alloy, the frequencies satisfying Eq. (7) are up to 14 kHz; for titanium the range is up to 4.7 kHz; for stainless steel, the range is up to 1500 Hz; for tungsten the range is up to 73 kHz. In these frequency ranges, the fluid loading will influence the mechanical properties of the foil.

In Figure 5 it can be observed that the noise generated by the rigid trailing edge is the highest. Due to the rigidity, there is strong interaction between the turbulence and the edge, making the trailing edge an efficient sound scatterer. The trailing edges made of aluminium alloy, stainless steel and tungsten all generate trailing edge noise lower than the rigid edge due to the elasticity under the influence of the heavy fluid. The influence of the heavy fluid is particularly significant at frequencies below 1 kHz. The lowest sound pressure spectrum is obtained for the low-stiffness aluminium alloy and tungsten trailing edges. A 30 dB reduction can be obtained at frequencies less than 1 kHz compared to the case

of a rigid edge. Although the tungsten has a high fluid loading parameter, the reduction of the trailing edge noise is very similar to the aluminium alloy edge due to its lower coincident frequency. If a fully clamped trailing edge is used, the edge noise will increase significantly, as shown in Figure 5 for a fully clamped aluminium alloy edge. A large reduction for a free edge compared to a clamped edge for the aluminium alloy can be observed.

A comparison of the radiated sound from the elastic and rigid plates can be obtained in terms of the ratio of the corresponding sound powers. The sound power is calculated by the surface integration of $\Phi(\omega)/\rho_0 c_0$ using a large radius $|\mathbf{x}|$ where $\Phi(\omega)$ is calculated using Eq. (1) for a rigid edge and Eq. (6) for an elastic edge. The ratios of the sound power generated by the different elastic edges to that from the rigid edge are shown in Figure 6. It can be seen that the reduction of trailing edge noise due to flexibility increases with a decrease in frequency. The biggest reduction is obtained by the material tungsten. The rate of the noise reduction as a function of frequency is the same for all materials studied. For a clamped aluminium alloy edge, a much smaller reduction of the elastic edge noise occurs.

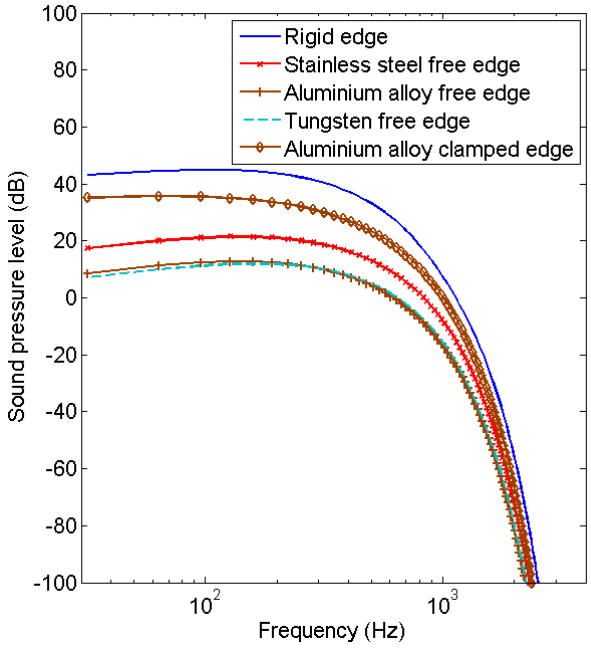

Figure 5 – Sound pressure spectrum at $x_1 = 0,\ x_2 = 0,\ x_3 = 1.2$ for different trailing edges

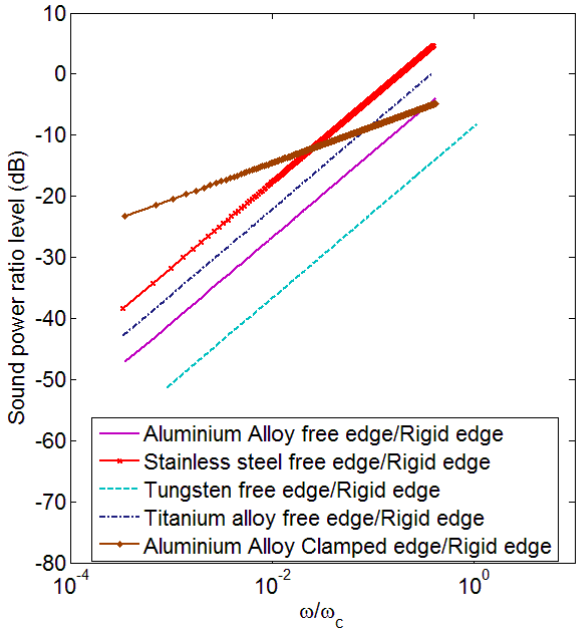

Figure 6 – Sound power ratio level for different trailing edges

It is important to note that the sound radiated by the plate flexural waves from the other parts of structure other than the trailing edge is not considered in this work. The reduction of edge noise due to the elasticity may be offset by the structure-borne noise, which is generated by the structural vibration excited by the turbulent flow over the trailing edge. It can be illustrated by a so-called radiation efficiency which is defined by the ratio of the scattered sound by the edge as given by Eq. (6) and the total flexural wave power excited by the turbulent flow, which can be obtained from the solution of Eqs. (4) and (5) and is a function of the fluid loading parameter and coincident frequency (24). The radiation efficiency is a mechanical property of the structure. For a foil with a free edge and a fluid loading parameter falling into a range as $0.1<\varepsilon<0.4$, the radiation efficiency is given by $\left(\omega/\omega_c\right)^{\left(5\varepsilon^{0.05}-2\right)}e^{-2.7\varepsilon^{0.2}}$; for a fully clamped edge, the radiation efficiency is equal to $\left(\omega/\omega_c\right)^{1.275}e^{-1.84\varepsilon}$ (24). The materials studied in this paper all satisfy the condition of $0.1<\varepsilon<0.4$, with the exception of tungsten. Figure 7 illustrates the radiation efficiency of different elastic edges using these formulas. In this study, aluminium alloy with a free edge has the lowest radiation efficiency and as such generates the lowest trailing edge noise. It can be seen that the power of the scattered edge noise is only a small proportion of the total structural flexural wave power, particularly for a free edge. Figure 7 also shows that a flexible structure with a clamped edge will be a more efficient trailing edge sound source than a structure with a free edge. Thus there is potential for the rest of the flexural wave power to be scattered into acoustic power by ribs or other structural discontinuities of the foil. Therefore detailed information of the structure is required to be able to make a full comparison between flow noise from rigid and elastic foils.

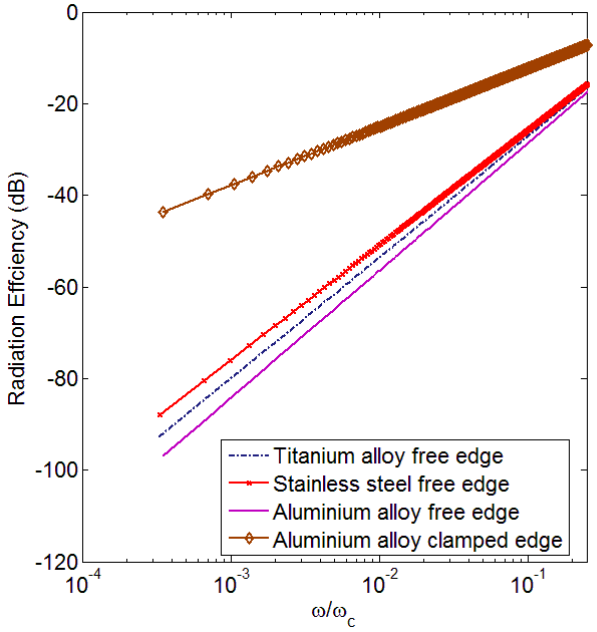

Figure 7 – Radiation efficiency for different trailing edges

5. CONCLUSIONS

Trailing edge noise is predicted using a hybrid method corresponding to the combination of a CFD solution and an acoustic analogy. The effect of material elasticity on the trailing edge noise is studied. The surface pressure spectrum near the trailing edge is calculated using the results of CFD simulations and shows multiple dependences on the frequency. For a NACA0015 foil in water, the trailing edge noise is reduced due to the elasticity of different materials considered in this study compared with the noise from a rigid edge. The highest reductions in trailing edge noise are obtained by foils constructed from the lower bending stiffness in the group of materials studied and which have a free end condition. For those cases, the fluid loading parameter is the highest and the heavy fluid loading changes the mechanical properties of the foil. However, any stiffening or reinforcement of these edges, for example, due to the use of clamped edges compared with free edges, results in an increase in radiated sound. The reduction of the trailing edge noise due to the elasticity can be further offset by the structure-borne radiated sound due to the flexible vibration of the plate, which is also excited by the

turbulent flow. To comprehensively study the noise generated by turbulent flow of an elastic hydrofoil, the flow-structure coupling and structure-borne radiated noise from the vibrating hydrofoil need to be taken into account.

REFERENCES

1. Wang M, Freund JB, Lele SK. Computational prediction of flow-generated sound. An Rev Fluid Mech. 2008;38:483-512.
2. Sandberg R, Sandham ND. Direct numerical simulation of turbulent flow past a trailing edge and the associated noise generation. J Fluid Mech. 2008;596:353-385.
3. Gloerfelt X. The link between wall pressure spectra and radiated sound from turbulent boundary layer. Proc 16th AIAA/CEAS AeroAcoustics Conference, AIAA paper 2010-3904, June 2010; Stockholm, Sweden.
4. Casalino D, Jacob M. Prediction of aerodynamic sound from circular rods via spanwise statistic modelling. J Sound Vib. 2003;262:815-844.
5. Casalino D. An advanced time approach for acoustic analogy predictions, J Sound Vib. 2003;261:583-612.
6. Wang M, Moin P. Computation of trailing-edge flow and noise using large-eddy simulation, AIAA J. 2000;38(12):2201-2209.
7. Crighton DG. Basic principles of aerodynamic noise generation. Prog Aero Sc. 1975;16(1):31-96.
8. Lighthill MJ. On sound generated aerodynamically. Part I: General theory. Proc Roy Soc Lon A. 1952;211:564-587.
9. Lighthill MJ. On sound generated aerodynamically. Part II: Turbulence as sound source. Proc Roy Soc Lon A. 1954;222:1-32.
10. Curle N. The influence of solid boundaries upon aerodynamic sound. Proc Roy Soc Lon A. 1955;231:505-514.
11. Wang M, Lele SK, Moin P. Computation of quadrupole noise using acoustic analogy. AIAA J. 1996;34(11):2247-2254.
12. Chase DM. Modelling the wavevector-frequency spectrum of turbulent boundary layer wall pressure. J Sound Vib. 1980;70(1):29-67.
13. Blake WK. Mechanics of Flow-Induced Sound and Vibration, Vols. I and II. Academic Press, Orlando, 1986.
14. Jaworski JW, Peake N. Parametric guidance for turbulent noise reduction from poroelastic trailing edges and owls. Proc 19th AIAA/CEAS Aeroacoustics conference, AIAA paper 2013-2007, May 2013; Berlin, Germany.
15. Jaworski JW, Peake N. Aerodynamic noise from a poroelastic trailing edge with implications for the silent flight of owls. Proc 18th AIAA/CEAS Aeroacoustics Conference, AIAA paper 2012-2038, June 2012; Colorado, USA.
16. Atassi HM, Kozlov A. Fluid loading in structural acoustics of an elastic airfoil, Proc 18th AIAA/CEAS Aeroacoustics Conference, AIAA paper 2012-2111, June 2012; Colorado, USA.
17. Howe MS. Acoustics of fluid–structure interactions. Cambridge University Press, 1998.
18. Chen L, MacGillivray IR. Prediction of trailing-edge noise based on CFD RANS solution. AIAA J. 2014;in press.
19. Brooks TF, Hodgson TH. Trailing edge noise prediction from measured surface pressures. J Sound Vib. 1981;78(1):69-117.
20. Ahn B. Unsteady wall beneath turbulent boundary layers. PhD Thesis, University of Cambridge, UK, 2005.
21. Blake WK. Turbulent boundary layer wall-pressure fluctuations on smooth and rough walls, J Fluid Mech. 1971;44(4):637-660.
22. Howe MS. Acoustics of fluid–structure interactions, Cambridge University Press, 1998.
23. Howe MS. Structure and acoustic noise produced by turbulent flow over an elastic trailing edge. Proc Roy Soc Lon A. 1993;442:533-554.
24. Howe MS. Sound produced by an aerodynamic source adjacent to a partly coated, finite elastic plate. Proc Roy Soc Lon A. 1992;436:351-372.
25. Do T, Chen L, Tu JY. Numerical study of turbulent trailing edge flows with base cavity effects using URANS. J Fluids Struct. 2010;26:1155-1173.
26. Benham PP, Crawford RJ. Mechanics of Engineering Materials, Longman Scientific & Technical, 1987, Longman Group Limited 1996.